

Published in final edited form as:

*Eur J Pharm Biopharm.* 2011 November ; 79(3): 526–536. doi:10.1016/j.ejpb.2011.06.007.

## pH-Responsive Nanoparticles Releasing Tenofovir for The Prevention of HIV Transmission

Tao Zhang<sup>a</sup>, Timothy F. Sturgis<sup>b</sup>, and Bi-Botti C. Youan<sup>a,\*</sup>

<sup>a</sup> Laboratory of Future Nanomedicines and Theoretical Chronopharmaceutics, Division of Pharmaceutical Science, University of Missouri-Kansas City, Kansas City, Missouri 64108

<sup>b</sup> Department of Environmental Health and Safety, University of Missouri-Kansas City, Kansas City, Missouri 64110

### Abstract

This study is designed to test the hypothesis that Tenofovir(TNF) or tenofovir disoproxil fumarate (TDF) loaded nanoparticles (NPs) prepared with a blend of poly(lactic-*co*-glycolic acid) (PLGA) and methacrylic acid copolymer (Eudragit<sup>®</sup> S-100, or S-100) are noncytotoxic and exhibit significant pH-responsive release of anti-HIV microbicides in presence of human semen. After NPs preparation by emulsification diffusion, their size, encapsulation efficiency (EE%), drug release profile, morphology, and cytotoxicity are characterized by dynamic light scattering, spectrophotometry, transmission electron microscopy, and cellular viability assay/trans epithelial electrical resistance measurement, respectively. Cellular uptake was elucidated by fluorescence spectroscopy and confocal microscopy. The NP shave an average size of 250 nm, maximal EE% of 16.1% and 37.2% for TNF and TDF, respectively. There is a 4-fold increase in the drug release rate from 75% S-100 blend in the presence of semen fluid simulant over 72 hr. At a concentration up to 10 mg/ml, the PLGA/S-100 NPs are noncytotoxic for 48 hr to vaginal endocervical/epithelial cells and *Lactobacillus crispatus*. The particle uptake (~50% in 24hr.) by these vaginal cell lines mostly occurred through caveolin-mediated pathway. These data suggest the promise of using PLGA/S-100 NP as an alternative controlled drug delivery system in intravaginal delivery of an anti-HIV/AIDS microbicide.

### Keywords

pH-responsive; nanoparticles; tenofovir; tenofovir disoproxil fumarate; topical delivery; HIV/AIDS microbicide

### 1. Introduction

According to the recent report of the global AIDS epidemic, it was estimated that there were 2.7 million new infections, and 2.0 million HIV/AIDS related deaths, in 2008[1].

Unprotected, heterosexual, vaginal intercourse has become one of the major routes of infection. Although the global percentage of women among people living with HIV has

© 2011 Elsevier B.V. All rights reserved.

\*Corresponding Author: Laboratory of Future Nanomedicines and Theoretical Chronopharmaceutics, Division of Pharmaceutical Science, University of Missouri-Kansas City, 2464 Charlotte, Kansas City, Missouri 64108, Tel: 816-235-2410; fax: 816-235-5779, youanb@umkc.edu).

**Publisher's Disclaimer:** This is a PDF file of an unedited manuscript that has been accepted for publication. As a service to our customers we are providing this early version of the manuscript. The manuscript will undergo copyediting, typesetting, and review of the resulting proof before it is published in its final citable form. Please note that during the production process errors may be discovered which could affect the content, and all legal disclaimers that apply to the journal pertain.

remained stable (50%), women are considered more susceptible to sexually-acquired HIV infection due to physiological, social, and economical factors [1]. Several HIV transmission prevention methods, such as condoms and circumcision, have been implemented, especially in developing countries. However, the results have been unsatisfactory, since it was reported in many regions that men were reluctant to use either method [2; 3]. Besides these facts, a successful HIV vaccine has yet to be developed. It is critical to design a topical delivery strategy of microbicides that women can use as a pre-exposure prophylaxis (PrEP) method. Some examples of new drug delivery system(DDS) designed for the delivery of anti-HIV drugs have been reported[4; 5; 6], but none of them are currently used clinically for the purpose of the prevention of HIV transmission.

Extensive research activities have been dedicated to the field of HIV microbicides development, such as detergents/pH buffers [7], entry/fusion inhibitors [8], and HIV reverse transcriptase inhibitors[9; 10]. Tenofovir (TNF, {[*(2R)*-1-(6-amino-9*H*-purin-9-yl)propan-2-yl]oxy }methylphosphonic acid) is a nucleotide analog HIV reverse transcriptase inhibitor whose prodrug (Tenofovir disoproxil fumarate, TDF) is now marketed in an oral dosage form (Viread<sup>®</sup>, Gilead Science), and its 1% vaginal gel formulation has recently been proven effective in clinical trial[11]. Other vaginal delivery strategies of tenofovir along with dapivirine and emtricitabine have also been studied [12; 13]. However, factors affecting the acceptability of the gel formulation include the ease of incorporation into typical sexual practices, and type of sexual partnership[14]. The vaginal route has been a site of local delivery as well as systemic delivery. Several dosage forms have been investigated as vaginal delivery systems, such as vaginal rings [15; 16], films[17], and gels [13]. Nanoparticles (NP) also potentially provide one possibility of such drug delivery system due to their unique characteristics, such as small size, protection of native drug, ability to reduce irritation at delivery site, and the ability of targeted delivery and controlled release of drugs. The concept of so called “nanomicrobicides” has embraced the advanced potential of nanomedicine, and efforts have been made to address major health problem of HIV prevention [18; 19]. Several insightful studies of NP vaginal formulation have indicated that it is a promising strategy toward the delivery of peptides and even siRNA [20; 21].

Since the HIV virus can be present in human semen during the intercourse, it is promising to design a semen-triggered topical delivery system. The ambient human vagina pH varies from 4–5, where as human semen has a higher pH (typically 7.5) as well as higher buffer capacity [22]. Therefore, the local acidic pH will be altered during intercourse, which has been utilized in semen triggered delivery and pH sensitive hydrogel [23]. However, vaginal retention of such a delivery system is also important. Otherwise, the short duration of the drug requires the user to apply microbicide formulation hours before sex (coital dependence), which leads to significant patient compliance issues as recently observed in the clinical trial of tenofovir gel [11; 14]. Based on the above consideration, the focus has been given to the preparation of a semen-triggered delivery system having a sustained release characteristic for vaginal delivery. It is hypothesized that a semen-triggered polymeric nanoparticulated delivery system, using poly(lactic-*co*-glycolic acid) (PLGA) and the methacrylic acid copolymer PLGA is a FDA-approved and widely accepted biodegradable copolymer used in NP formulation, which can also provide the sustained release of an encapsulated drug. Various blends of Eudragit<sup>®</sup> and PLGA have been described in the preparation of heparin[24], antibiotics [25; 26], gene encoding mouse interleukin-10[27], salmon calcitonin[28] and diclofenac sodium[29]loaded nanoparticles. Eudragit<sup>®</sup> S-100 (hereafter referred to as S-100), would be effective and safe *polymeric matrix* in the prevention of HIV transmission by vaginal route. Basically, S-100 is a methacrylic acid - methyl methacrylate copolymer (1:2) synthesized from methacrylic acid and methacrylic acid methyl ester, which is soluble in an alkaline environment [30]. Therefore, it has been widely used in intestine or colon delivery systems where pH is above 7 [30]. The present

investigation is aimed at testing the hypothesis that Tenofovir tenofovir disoproxil fumarate loaded nanoparticles prepared with a blend of poly(lactic-co-glycolic acid) (PLGA) and methacrylic acid copolymer (S-100) are noncytotoxic and exhibit significant pH-responsive release of anti-HIV microbicides in presence of human semen. Basically, the TNF and TDF loaded, pH-sensitive NP was prepared, and physicochemical characteristics, as well as biological responses, were investigated. The results of this study demonstrates that a PLGA/S-100 NP formulation may provide semen-triggered delivery and sustained release of an encapsulated microbicide for the prevention of HIV/AIDS transmission.

## 2. Materials and methods

### 2.1. Materials

Tenofovir (TNF) was purchased from Zhongshuo Pharmaceutical Co. Ltd. (Beijing, China). Tenofovir disoproxil fumarate (TDF) was obtained through the AIDS Research and Reference Reagent Program, Division of AIDS, NIAID, NIH, Rockville, Maryland. Poly(D, L-lactide-co-glycolide) Resomer<sup>®</sup> RG756 with L/G ratio of 75:25 (MW 76-116kDa) was purchased from Boehringer Ingelheim Inc. (Ingelheim, Germany). Eudragit<sup>®</sup> S-100 or S-100(Methacrylic acid-methyl methacrylate copolymer 1:2) was purchased from *Evonik Industries* (Darmstadt, Germany). Poloxamer 407 (Pluronic<sup>®</sup> F127) was a gift from the BASF Corporation (Rhom, Germany). Coumarin-6, propidium iodide (PI) and dimethyl sulfoxide (DMSO) were purchased from Sigma Aldrich (St. Louis, MO, USA). CytoTox-ONE<sup>™</sup> and CellTiter 96<sup>™</sup> Aqueous kits were purchased from Promega (Madison, WI, USA). All other chemicals used in this study were of analytical grade and used without further purification.

### 2.2. Nanoparticle Preparation

TNF and TDF loaded PLGA/S-100 nanoparticles were prepared at room temperature using a previously described emulsification solvent diffusion method [31]. Briefly, TNF (5 mg) and the polymer (100mg, PLGA/S-100 ratio 25:75, 50:50 and 75:25) were co-dissolved in 4 ml DMSO. This mixture served as the organic phase for the NP preparation. The organic phase was added dropwise to 25 ml of aqueous phase, containing 0.6% (w/v) Pluronic F127, under homogenization at 13,500 rpm for 10 min (IKA ULTRA-TURRAX T-25, Staufen, Germany). The suspension was further ultracentrifuged at 15,000 rpm for 1 hr (Beckman L8-70 M Ultracentrifuge, Brea, CA, USA) to collect NP, and then washed three times with distilled water to remove the surfactant. The supernatant was used for the determination of drug encapsulation efficiency (EE%). Finally, the NPs were first frozen in liquid nitrogen then lyophilized for 12 hr using a lab-scale freeze dryer (Labconco Corporation, Kansas City, MO, USA) under  $-46^{\circ}\text{C}$ , and stored at  $4^{\circ}\text{C}$  until use. Blank NP and Coumarin-6 (C-6) loaded PLGA/S-100 NP were prepared using the same method.

### 2.3. Nanoparticle Characterization

**2.3.1. Particle Size and Zeta Potential**—The particle size and size distribution of the various NP solutions were measured at  $25^{\circ}\text{C}$  by dynamic light scattering method (Zetasizer Nano ZS, Malvern Instruments Ltd, Worcestershire, UK). The particle size of the different samples (nanosuspension before lyophilization and suspension of lyophilized NP powder) were evaluated and represented as Z-average diameter. The zeta potential of the PLGA/S-100 NP suspension was measured using the zeta potential analysis mode of the instrument. Nanosphere<sup>™</sup> size standard ( $59\pm 2.5$  nm) and zeta potential standard ( $-68\pm 6.8$  mV) were used to calibrate the instrument prior to the analysis.

**2.3.2. Morphology**—The images of the NP formulation were taken by transmission electron microscopy (TEM). Particles were diluted in 2.5% uranyl acetate (UA), sonicated,

and then 8 $\mu$ L of the solution was put on a carbon coated grid and allowed to equilibrate for 5min; excess solution was wicked off. Then 5% UA was put on the grid to increase contrast. The grids were viewed under a JEOL JEM 1400 Transmission Electron Microscope (JEOL Inc., Peabody, USA), and photographed digitally with a Gatan axis-mount 2k $\times$ 2k digital camera.

**2.3.3. Encapsulation Efficiency**—The encapsulation efficiency (EE%) was measured at a wavelength of 260 nm by UV spectrometer (Spectronic Genesys 10 Bio, Thermo Electron Corporation, WI, USA). The standard curves of TNF and TDF were prepared using drug concentration ranging from 2~100  $\mu$ g/ml. The amount of encapsulated drug was calculated using mass balance by subtracting the amount of the free drug present in the supernatant from the total drug amount initially added in the preparation medium.

**2.3.4. *In vitro* Release from PLGA/S-100 Nanoparticles**—To estimate the amount of drug released from the PLGA/S-100 NP and assess the rate of pH-responsiveness, an *in vitro* release study was conducted over 72 hr using a vaginal fluid simulant (VFS, pH 4.2 $\pm$ 0.1) and a semen fluid simulant (SFS, pH 7.6 $\pm$ 0.1). The components used in the VFS and SFS formulations are adopted from previous articles [22; 32]. Briefly, the VFS was prepared using sodium chloride, potassium hydroxide, calcium hydroxide, albumin bovine fraction V, lactic acid, glycerol, urea, acetic acid, glucose and water. The components of SFS were: sodium phosphate monobasic/dibasic, sodium citrate, potassium chloride, potassium hydroxide, fructose, glucose, lactic acid, urea, and bovine serum albumin. The samples tested included drug loaded NP with various weight ratios of S-100 to PLGA in the polymeric matrix. The release profile of TNF and TDF was also compared. Each experiment was run in triplicate, along with a blank control formulation. For this release study, 1 ml of the resuspended pellet after ultracentrifugation (corresponding to 250  $\mu$ g of encapsulated drug) was put into a Spectra/Por cellulose ester membrane dialysis bag (Spectra/Por Float-A-Lyzer G2, MWCO 3.5–5 KD, Spectrum Laboratories Inc. Rancho Dominguez, CA, USA), and maintained in 40 ml of release medium using a shaking water bath (BS-06 Lab. Companion, Jeio Tech Co., LTD, Seoul, Korea) at 37  $^{\circ}$ C with an agitation speed of 60 rpm. In order to test the pH-responsiveness, VFS alone, and 1:4 ratio of VFS/SFS mixture (final pH 7.57), were used as release medium. Owen et. al. reported that the volume of normal human vaginal fluid is 0.75 ml, and the volume of human ejaculate is 3.4 ml [22; 32]. At predetermined time intervals, 1 ml of buffer solution outside the dialysis bag was removed and replaced with 1 ml of fresh buffer. The amount of drug released was measured by a UV spectrometer at 260 nm as described previously. The standard curve was prepared using the same method as in the previous section. The standard curve was  $y=0.0446x+0.0052$  ( $R^2=0.9993$ ) for TNF and  $y=0.0209x+0.0215$  ( $R^2=0.9998$ ) for TDF.

## 2.4. Cell Culture

Human vaginal epithelial cell line (VK2/E6E7, ATCC Number CRL-2616), Human Endocervical epithelial cell line (End1/E6E7, ATCC Number CRL-2615), and *Lactobacillus crispatus* (ATCC Number 33197) were obtained from the American Type Culture Collection (Manassas, VA, USA). Unless otherwise stated, culture medium and reagents were purchased from Invitrogen (Carlsbad, CA, USA). VK2/E6E7 and End1/E6E7 cells were grown and routinely maintained at 37  $^{\circ}$ C in 75-cm<sup>2</sup> culture flasks, in keratinocyte-serum free medium supplemented with 0.1 ng/ml human recombinant EGF, 0.05 mg/ml bovine pituitary extract, additional calcium chloride 44.1 mg/L, and in atmosphere of 5% CO<sub>2</sub>. *Lactobacillus crispatus* was grown in an ATCC medium 416 *Lactobacilli* MRS broth (BD, Franklin Lakes, NJ, USA) at 37 $^{\circ}$ C.

## 2.5. Cytotoxicity Studies

**2.5.1. Cytotoxicity Studies on Vaginal/Endocervical Cell Lines**—Cell viability was determined by a DTX 800 multimode microplate reader (Beckman Coulter, Brea, CA, USA). Cells were transferred to 96-well plates to ensure  $1 \times 10^4$  cells per well, and were allowed to grow until they reached 80% confluence. Then the medium was changed with 100  $\mu$ l medium of blank PLGA/S-100 NP with different PLGA to S-100 ratios. The concentration of NP in the cell culture medium ranged from 25  $\mu$ g/ml to 10,000  $\mu$ g/ml. The average size of 100% S-100 NP used in cytotoxicity study was 535.8 nm. The plates were incubated for 24 and 48 hr. The medium was used as a negative control and 1% Triton X as a positive control. Twenty microliters of [3-(4,5-dimethylthiazol-2-yl)-5-(3-carboxymethoxyphenyl)-2-(4-sulfophenyl)-2H-tetrazolium] solution (MTS, CellTiter 96<sup>TM</sup> Aqueous, Promega, Madison, WI, USA) was added to each well and incubated for 1 hr at 37°C. Cell viability was determined using equation (1):

$$Viability(\%) = \frac{ABS_{Test}}{ABS_{Control}} \times 100 \quad (1)$$

where  $ABS_{Test}$  and  $ABS_{Control}$  represented the amount of formazan detected in viable cells.

The cellular membrane integrity was determined by the release of lactate dehydrogenase (LDH). Briefly, cells were seeded in 96-well plates and incubated with PLGA/S-100 NP using the same condition as stated above. One row of the 96-well plate without cells was used to determine the background fluorescence that might be present. At different time intervals, the plates were equilibrated at 22°C and 100  $\mu$ l of CytoTox-ONE<sup>TM</sup> reagent (Promega, Madison, WI, USA) was added to each well. The plate was incubated at 22°C for 10 min, and then 50  $\mu$ l of stop solution was added to each well. The fluorescence was detected using the above microplate reader at excitation wavelength of 560 nm and emission wavelength of 590 nm. The percent cytotoxicity for a given treatment can be expressed using equation (2):

$$Cytotoxicity(\%) = 100 \times \frac{Experimental - Background}{Positive - Background} \quad (2)$$

where Experimental, Background, and Positive represent the absorbance of NP-treated wells. The background control wells contained cells not treated with NP, and positive control wells contained cells treated with 1% Triton X, respectively.

**2.5.2. Lactobacillus Viability Assay**—To assess the effect of PLGA/S-100 NP on *L. crispatus* growth, the viability assay was performed using aMTS assay. The soluble tetrazolium salt method has previously been tested on various Gram-positive and Gram-negative bacteria including *Lactobacillus*, showing linear relationships between the absorbance and viable microbial cell density [33]. Briefly, the bacteria density was adjusted to an  $OD_{670}$  of 0.06, which corresponds to a 0.5 McFarland Standard or  $10^8$  CFU/ml [34]. *L. crispatus* was seeded in 96-well plates at a volume of 100  $\mu$ l and incubated with 100  $\mu$ l of a series of NP dilutions at 37°C for 24 and 48 hr. Bacterial wells treated with commercially available Penicillin-Streptomycin solution (Invitrogen, Carlsbad, CA, USA) at 10  $\mu$ g/ml were used as positive controls. After incubation, a 20  $\mu$ l MTS reagent was added to each well and the bacterial viability was determined by measurement of the  $OD_{490}$  using the microplate reader. The percent viability was expressed using equation (1).

**2.5.3. Transepithelial Electrical Resistance (TEER) Measurement**—To determine the effect of PLGA/S-100 NP on the epithelial integrity, the transepithelial electrical resistance (TEER) was measured. Polycarbonate transwell inserts (Corning Costar

Transwell dual-chamber system, Fisher Scientific) were coated with 0.05% type IV collagen (Sigma) prepared in 0.2% acetic acid and 7.5% ethanol overnight at 37°C, 5% CO<sub>2</sub>. End1/E6E7 cells ( $4 \times 10^5$ ) were seeded onto the coated transwell inserts and grown in a 12-well dual chamber system for seven days to achieve polarization. At that time, PLGA/S-100 NP (75% S-100 at 1,000 or 10,000 µg/ml) was added to the apical surface of the monolayer, and TEER was measured at 30 min, 1, 2, 4, and 24 hr using an EVOM voltmeter (World Precision Instruments, Sarasota, FL, USA). As controls, wells treated with medium, cells treated with Triton X, or no cells were used. The TEER was expressed as ( $\Omega \times \text{cm}^2$ ) value of the treated wells subtracting that of the cell free wells.

## 2.6. Cellular Uptake Studies

Cellular uptake studies were performed as previously described[35]. The cells ( $1 \times 10^4$ ) were seeded in the 96-well plates. After 80% confluence was reached, the cells were incubated with C-6 NP suspension (250, 500, and 1,000 µg/ml in medium) for 4, 24, and 48 hr. Cells treated with medium only were used as background, and control was kept by adding C-6 NP suspension to the cell-free wells. At different time intervals, suspension was removed and the cells were washed three times using a phosphate buffer saline (PBS, pH=7.4) solution. After adding 1% Triton X for cells lysis, the fluorescence of the plate was measured using a Cary Eclipse fluorescence spectrophotometer (Varian Inc., Palo Alto, CA, USA). The excitation and emission wavelengths were 430 and 485 nm, respectively. The cellular uptake efficiency was calculated by the ratio of the fluorescence intensity in the cell coated wells to those in control wells.

For the confocal microscopy experiment, cells were grown on a 16-well Culture Well™ chambered coverglass (Grace Bio-Labs, Inc., Bend, OR, USA). After 80% confluence was reached, medium was substituted with 100 µl C-6 NP suspension (250 µg/ml). After incubation for 4hrs, the suspension was removed and 10 µl of 70% ethanol was used to fix the cells at 37°C for 20 min. Ethanol solution was then removed and the cells were washed three times using PBS. Ten µl of propidium iodide (PI, 5mg/ml) was added to stain the nucleus for 30 min. After the PI was washed three times using PBS, the coverglass was separated and observed by a confocal laser scanning microscope using a 40x water lens with a KrAr laser (Zeiss LSM 410) and Fluoview FV300 software. The elucidation of the mechanism of the NPs endocytosis was done through uptake inhibition assay previously described [36]. Cytoskeleton recognition was prevented by incubation the cells with cytochalasin D (10 µg/ml) for 30 min followed by C-6 NP application. Macropinocytosis was promoted through pre-incubation with phorbol myristate acetate (PMA, 1 µM) for 30 min followed by C-6 NP. Clathrin-dependent endocytosis was inhibited by co-treatment C-6 NP with chlorpromazine (10 µg/ml) after the pre-incubation at the same concentration. Finally, the caveolin-mediated endocytosis was disturbed by pre-incubate the cells with genistein (200 µg/ml) for 30 min followed by co-treatment with C-6 NP at the same concentration. Cells treated with C-6 NP alone were used as control. After 24 hours, cells were analyzed as described in the previous section.

## 2.7. Data Analysis

After triplicate experiments, data were expressed as mean  $\pm$  standard deviations. Compare to controls, the statistical significant difference of a given mean was determined using a t-test. A P value <0.05 was considered statistically significant.

### 3. Results

#### 3.1. Physicochemical characteristics of TNF or TDF loaded PLGA/S-100 NP

The size, EE%, PDI, and zeta potential of TNF/TDF loaded PLGA/S-100 NPs are listed in Table 1. Fig. 1A shows a typical size distribution of the NP sample. As shown in Fig. 1B, the morphology of drug-loaded NPs appeared to be spherical in shape and smooth in surface. There is variance in size distribution, as shown in a PDI value greater than 0.005, but the majority of the particles have a diameter below 300 nm. The encapsulation efficiency of TNF is less than 20%. The EE% of TDF is significantly higher than that of TNF (P value = 0.008, 0.004, 0.005 for NP with S-100/PLGA ratio of 25/75, 50/50 and 75/25, respectively). The EE% decreases with increasing S-100 percentage for both TNF and TDF.

#### 3.2. *in vitro* release study

The *in vitro* drug release for a period of 72 hrs in VFS and the mixture of VFS/SFS are shown in Fig. 2A to D. For NP with a 75% S-100/25% PLGA weight ratio, there is a 43.6±5.0% and a 78.5±5.8% of the total amount of TNF released in 24 and 72 hrs under pH 7.6, respectively; while there's only 19.6±4.3% of the total TNF release in 72 hrs under pH 4.2 (Fig. 2A). By reducing the amount of S-100 in that of total polymers, the drug release rate also decreases (Fig. 2B and C). The release rate of TNF and TDF from a 75%/25% S-100/PLGA weight ratio NP under pH 7.6 is also compared (Fig. 2D). The release rate of TDF is lower compared to TNF.

#### 3.3. Cytotoxicity study

**3.3.1. Effect of PLGA/S-100 NP on viability of epithelial cell lines**—Our data suggest that a PLGA/S-100 blend NP is safe in both vaginal (VK) and endocervical (Endo) epithelial cell lines up to 10 mg/ml (Fig. 3A through D). Significant reduction of cell viability ( $p < 0.05$ ) has been observed for pure Eudragit® S-100 NP at 10 mg/ml on VK cell line after 24 (77.34±7.15%) and 48 hr (71.76±10.60%). This effect is observed on all three formulations (S-100/PLGA 50/50%, 75/25%, 100/0%) at 10 mg/ml on Endo cells. Lactate dehydrogenase (LDH) assay estimates the cell membrane integrity and the release of LDH are markers of non-viable cells. The results of the LDH study correlate with that of the MTS study (Fig. 4A through D). PLGA/S-100 NP shows a more toxic effect on Endo cells than VK cells, especially for NP with high S-100 ratio under high concentration (10 mg/ml). However, the highest percent of cell death observed in the whole study is 12.14±1.36% compared to positive control, suggesting a relatively minor toxic effect.

The TEER data is shown in Fig. 5. The medium treated wells varied by less than 13% of their TEER values in a period of 24hr. The two highest concentrations (1000 and 10,000 µg/ml) of the NP reduced the TEER of Endo cells by a maximum of 9% ( $p = 0.74$ ) and 18% ( $p = 0.76$ ), respectively, indicating a transient reduction of the monolayer integrity. Conversely, the cell monolayer loses its TEER value up to 80% in 24 hr in the positive control. Although there is some reduction of viability on Endo cells at high concentration as shown in the MTS study, the NP does not compromise the integrity of Endo cells monolayer.

**3.3.2. Effect of PLGA/S-100 NP on viability of vaginal flora**—Three PLGA/S-100 nanoformulations were tested on *L. crispatus* from 25 to 10,000 µg/ml for a period of 48 hr. No statistically significant loss of viability ( $P > 0.05$ ) was found (Fig. 6).

### 3.4. Cellular uptake study

Around 50% of the NP can be uptaken by cervicovaginal epithelial cells within 24 hr (See Fig. 7). The uptake process is further visualized and proven by a confocal microscope study. Cell nuclei are stained by propidium iodide (PI) and exhibit a red color under red channel while C-6 NP exhibits a green color under green channel. X-Y axis projections are performed using a 0.5  $\mu\text{m}$  interval in an 11 to 18  $\mu\text{m}$  range. Confocal microscopic images (Fig. 8) verify that nanoparticles are actually internalized by VK and Endo cells, and distribute throughout the cytoplasm and around nucleus instead of localized on the surface of the cells. The uptake inhibition study shows that the treatment with genistein, an inhibitor of caveolin-mediated endocytosis, has significant reduction of NP uptake on VK cells at all concentrations studied (Fig. 9). Interruption of actin microfilament polymerization and depolymerization by cytochalasin D results in significant reduction of uptake on NP concentrations of 250 and 1000  $\mu\text{g/ml}$ , but not on 500  $\mu\text{g/ml}$ . Clathrin-dependent endocytosis and micropinocytosis are not involved in PLGA/S-100 NP internalization as indicated by PMA and Chlorpromazine treated studies.

## 4. Discussion

PLGA/S-100 NP have an average size between 200–300 nm, which is comparable to previously reported particle size such as the Eudragit RS/RL NP [37] and Eudragit RS/PLGA blend NP, in which the obtained Eudragit RS/PLGA had an average size of 273 nm [24]. At the drug loading reported, the nanoparticles were spherical and smooth particles in shape. The impact of drug loading on the NPs morphology remained to be elucidated. The measured zeta potential was around  $-3.0$  mV. This relatively weak negative charge on the surface could be attributed to the presence of ionized carboxyl groups on the particle surface, which is present in both PLGA and S100. The size and zeta potential of the NP can affect toxicity and stability, as well as tissue uptake and interstitial trafficking [38]. It was shown that topical administration of PLGA NP with a strong negative charge (around  $-20$  mV) and size around 200 nm, can display greater permeability deep into vaginal epithelium as well as into the ectocervical tissue [20; 21]. Therefore a close-to-neutral charge and relatively larger size, as obtained in this study, would help reduce particle traversing through the reproductive tract tissue, thus forming a first line of defense of pH-sensitive NP for effective prevention of HIV transmission. Tenofovir is highly hydrophilic (Log P =  $-1.6$ ) [39], and therefore it most likely partitions into the aqueous phase during NP preparation, with the incorporation of increasing proportion of the relatively more hydrophilic polymer S-100 into the nanoformulation. TDF has higher EE% because it is more hydrophobic (Log P = 1.25) compared to TNF [40], and it also has a higher molecular weight (635.52 vs. 287.03 g/mol for TNF) [39; 40]. In addition to low molecular weight and relative water solubility of the drug, the high specific surface area of the NPs could have also contributed to the low EE%. The result of this study suggests that this drug delivery template works better for the hydrophobic microbicide, and further study is needed to either improve the EE% of the hydrophilic drug, or develop this system using hydrophobic microbicides.

It was hypothesized that the presence of S-100 in the polymeric matrix accelerates the drug release rate in the presence of the semen fluid simulant following a combination of several fundamental mechanisms. Firstly, the importance of type of drug and device geometry in PLGA-based drug delivery systems is well established [41]. Although the initial NPs appear to be similar, the difference in particle geometry may be consecutive to the solubilization of the various proportions of the pH-sensitive polymer (S-100). Secondly, the microenvironmental pH is also known to significantly impact the stability and release of compounds [42]. In small size microspheres (2  $\mu\text{m}$  in diameter), the water soluble acids generated by PLGA degradation hydrolysis were likely able to diffuse out close to edge of microspheres therefore displaying a more neutral internal pH [43]. These NPs being smaller is



size, it is reasonably speculated that the internal pH is neutral as well. In this study, Eudragit® S-100 was selected instead of L-100 because its triggering pH for solubilization is closer to that of VFS/SFS mixture (final pH 7.57) so ensure triggered release by SFS and avoid premature drug release in case of relatively higher vaginal pH. The ester/acid group ratio ( $n_e/n_a$ ) is approximately 2 for Eudragit® type S, and 1 for Eudragit® type L[29].[44] where  $n_a$  and  $n_e$ (groups/molecule) are the number of acidic and ester groups in a polymer molecule. Indeed, according to the manufacturer's product data sheet, the acid value of S-100 and L-100 is 190 mg and 315 mg KOH/g polymer. Because Eudragit® polymer type S is solubilized by ionization reactions of pendent carboxyl groups, its solubility decreases as the concentration of hydrogen ions in the solution increases. The polymer solubility is very low at pH values lower than the  $pK_a$  of the polymer ( $pK_a = 6$  for Eudragit® type S), but increases rapidly (approximately 17 fold) as the solution pH increases from 6 to 7, and then becomes independent of solution pH for pH values greater than 10.[44]. Optimum values of both a polymeric matrix's  $pK_a$  and a solution pH exist at which a maximum facilitated diffusion occurs and the overall polymer dissolution could change from diffusion-limited to disentanglement-limited process[44]. It remains to be elucidated whether the carboxylic acid groups in Eudragit® can accelerate PLGA degradation either in liquid or solid state. As previously demonstrated, human semen can be detected in vaginal tract up to 48 hours after intercourse, and the cervicovaginal pH remains at a relatively high level within the first 24 hours after the intercourse [45]. These observations provide a solid ground for the potential clinical relevance of the observed time dependent pH-responsiveness. Our data support this hypothesis since increasing the percentage of S-100 results in a higher drug release rate, and there is an approximate of 50% drug release within the first 24 hrs. Since the composition of the polymeric matrix is random in NP, lower amounts of S-100 will give the drug less of a chance to be in contact with the release medium. Therefore, the drug release rate might become more dependent on the PLGA degradation rate at a lower S-100 weight ratio. This can explain the similar release rate shown in Fig. 2C, since it has been shown that PLGA nanoparticles have a higher drug release rate in an acidic pH environment [20]. Tenofovir has two  $pK_a$  values at 3.8 and 6.7[39]. At lower pH, the ratio  $[HA]/[A^-]$  of unionized ([HA]) vs. ionized species ( $[A^-]$ ) is higher, which has been identified as a factor that could enhance the permeation of this drug through lipophilic membrane[39] based on pH-partition hypothesis. At higher pH, the degradation of PLGA is controlled by formation of acidic oligomers creating water channels[46]. On the other hand, low pH could catalyze the breakage of ester bond in the polymer backbone, which is considered to be a controlling effect of the zero-order release phase of PLGA NP[46]. The average  $pK_a$  of PLGA is 3.85 considering the  $pK_a$  of lactic acid of 3.86 and that of glycolic acid 3.83[47]. A drop in the pH of the release media will also cause an increase in the  $[HA]/[A^-]$  ratio, thus reducing the negative charge of PLGA. Reduced charge-charge interaction between PLGA matrix and the encapsulated drug could also contribute to the drug release at lower pH. It is also well known that the ratio of lactide to glycolide in PLGA strongly affects the degradation rate of PLGA [48]. As the hydrophobicity of PLGA increases, a slower drug release rate is observed because of the reduced water uptake in the PLGA matrix. Therefore by adjusting the PLGA composition and S-100 percentage, the release rate of TNF can be further controlled. Given the fact that TDF is more hydrophobic in nature [39; 40], the TDF release rate is more dependent on its diffusion rate through the polymeric matrix, while TNF is more exposed to the aqueous phase with release requiring only dissociation from the NP surface.

The actual drug loading for the 75%/25% S-100/PLGA weight ratio NP is 0.48% w/w for TNF and 1.20% w/w for TDF, which can be converted to 1.7  $\mu\text{mol}$  and 1.9  $\mu\text{mol}$  per 100 mg NP for TNF and TDF, respectively. It has been reported that the *in vitro*  $EC_{50}$  of TNF and TDF was  $5.0 \pm 2.6$  and  $0.05 \pm 0.03 \mu\text{M}$  [49]. Considering that a vaginal suppository weighs approximately 5g, and assuming a 20% w/w of NP in such a suppository, the

ultimate vaginal formulation, would be respectively loaded with 17 and 19  $\mu\text{mol}$  of TNF and TDF, leading to a vaginal drug concentration of 5.7  $\mu\text{M}$  and 6.3  $\mu\text{M}$ , given the fact that the average total volume of vaginal fluid and cervical mucus is 3 ml [50]. Therefore it can be reasonably speculated that a microbicide released from pH-sensitive NP would potentially exhibit an anti-HIV effect. However, this remains to be elucidated in the future *in vitro* and *in vivo* safety and efficacy assays taking into account composition-property performance relationships[51].

Another major concern for topical delivery of HIV microbicide formulation is the retention time of the formulation. It has been reported that PLGA nanoparticles loaded with Coumarin-6 can be observed throughout the reproductive tract up to 7 days after only a single vaginal application *in vivo*[21]. Therefore it is reasonably speculated that the proposed PLGA/S-100 NP has the ability to be retained locally in the vaginal cavity. However, this remains to be further confirmed by *in vivo* biodistribution and retention study.

Topical strategies to prevent HIV infection must have safety profiles that justify its application, especially on mucosal integrity and vaginal ecology [52]. Since a simple 1% tenofovir gel has been proven to be safe on epithelial cell lines and peripheral blood mononuclear cells (PMBCs) [11; 53], the purpose of this study is to test the effect of the vehicle PLGA/S-100 NP on the viability of epithelial cells. The observed difference in the viability profile between VK and Endo cells might be due to their difference in cell sensitivity. Columnar endocervical epithelial cells are thought to be more susceptible to toxicant and release more proinflammatory cytokines, such as interleukin 6, 7, and 8, when damaged than do vagina epithelial cells [54]. Being only a single cell layer, endocervical epithelium is more vulnerable to pathogen invasion and tissue injury. Therefore active cytokine production would enable a quick response to infections for maintenance of sterility of the region [55]. Based on the data of the MTS, LDH, and TEER studies, the overall toxic effect of PLGA/S-100 NP is transient, especially at concentrations lower than 10 mg/ml. By increasing the amount of PLGA, which is a biodegradable and biocompatible polymer, the cytotoxicity can be further reduced. By comparing the cytotoxicity data, PLGA/S-100 NP has a better safety profile than the carbopol gel formulation [23], and has a similar safety profile to that of the terpolymer [23] and hydroxyethylcellulose gel formulations[53]. For example, it has been reported that a pH-responsive terpolymer gel formulation can achieve almost 100% viability on a mouse fibroblast cell line at 10 mg/ml, but the viability of cells was less than 20% when treated with carbopol at the same concentration. It is noted that carbopol is widely accepted in commercial vaginal formulations at 0.5–20 mg/ml [56].

The normal vaginal flora consists of predominantly *Lactobacillus* species. It is critical that any microbicide formulation to not disturb this normal vagina flora. This is important to maintain the low pH environment and the secretion of hydrogen peroxide ( $\text{H}_2\text{O}_2$ ), which provides a natural barrier against HIV transmission [57]. *Lactobacillus crispatus* was used as a model bacteria since it has been proven to produce  $\text{H}_2\text{O}_2$ [58]. Our data suggested that PLGA/S-100 NP would not disturb the normal vaginal flora. Together with other safety data, PLGA/S-100 NP has the potential to be a safe matrix for vaginal delivery of microbicide. However, further studies are needed to rule out eventual unwanted inflammatory responses.

Nanoparticles encapsulating fluorescent dyes have been frequently used to study cellular uptake, and coumarin-6 was suggested to be a suitable marker for nanoparticles because of their low leaching percentage under various conditions [35]. Therefore the intracellular fluorescence of C-6 may not be attributed to the uptake of free coumarin-6 released from nanoparticles. A similar uptake pattern of PLGA NP in C6 glioma cells has been reported [35], suggesting the capability of endocytosis function of epithelial cells on the reproductive

tract. By applying different chemicals to inhibit/promote different endocytic pathways, it is possible to study the specific pathway involved in the internalization of PLGA/S-100 NP. The results indicate that caveolin-mediated endocytosis is clearly involved; with a maximum of 65% reduction observed under genistein treatment. Actin microfilament also contributed in the process, as evidenced by 42% and 36% reduction on 250 and 1000  $\mu\text{g/ml}$  NP, respectively. On the contrast, clathrin-dependent endocytosis is not involved in the internalization. It has been previously reported that the NP size can affect the pathways of internalization, with a cut-off of 200 nm. Particles under 200 nm are more likely to be internalized through clathrin-dependent endocytosis, and caveolin-mediated pathway favors particles over 200 nm [59]. Our data support this hypothesis since the PLGA/S-100 NP has an average size above 200 nm. However, multiple factors can affect NP internalization such as cell line dependence, particle size, and surface composition. Therefore, additional investigations are needed to further the subcellular fate of these NPs. It was demonstrated in the *in vitro* release study that over 40% of the drug can be released within the first 24 hours after a contact with the simulated semen. In the case when no sexual activity is immediately engaged, the proportion of NP that is uptaken by the vaginal epithelium would allow the sustained release of microbicide to the basal layer due to the intracellular polymer degradation. Based on our current understanding on how viruses enter animal cells [48], these findings would provide additional physicochemical barrier by outdistancing the virus in regions where the HIV has been shown to transmigrate and infect its target cells [52]. Therefore, these data are important, not only because they elucidate the fate of nanoparticles at site of action, but also reveal the possibility of microbicide localization at its site of action.

## 5. Conclusions

In this study, pH-responsive nanoparticles loaded with tenofovir or tenofovir disoproxil fumarate are formulated. The nanoformulation prepared by 75/25% ratio of S-100/PLGA matrix loaded with TDF (size 336.8 nm, encapsulation efficiency 24.0%, drug loading 1.9% w/w) appears to be the best formulation considering the overall effect based on drug loading, *in vitro* release (pH-responsive release), and safety (up to 10 mg/ml). PLGA/Eudragit S-100 nanoparticles have several advantages, such as small particle size, controlled release of drug in the presence of semen, and they are potentially safe to the vaginal physiological environment. However, the encapsulation efficiency is low. This might be increased by optimization of the preparation protocol or even using a more hydrophobic microbicides in the future study. Future studies are needed to characterize the conditions for optimal formulation stability, vaginal retention time, immunological/inflammatory responses, *in vivo* safety and efficacy. Collectively, these data suggest the possibility of using nanoparticles as a delivery system for intravaginal delivery of HIV microbicides for the prevention of HIV transmission.

## Acknowledgments

The authors would also like to thank the support from Dr. Jeffery Price (Associate Professor, School of Biological Sciences of University of Missouri-Kansas City for Confocal microscopic study, Dr. Elisabet Nalvarte (Research Associate Professor, Department of Oral Biology, University of Missouri-Kansas City, MO) for fluorescent spectrophotometer, and Louis Ross, Cheryl Jensen and Randy Tindall (Electron Microscopy Center, University of Missouri-Columbia, MO) for the electron microscopy. The work presented was supported by Award Number R21AI083092 from the National Institute of Allergy And Infectious Diseases. The content is solely the responsibility of the authors and does not necessarily represent the official views of the National Institute of Allergy And Infectious Diseases or the National Institutes of Health.

## ABBREVIATIONS

<b>C-6</b>	Coumarin-6
<b>MTS</b>	[3-(4, 5-dimethylthiazol-2-yl)-5-(3-carboxymethoxyphenyl)-2-(4-sulfophenyl)-2H-tetrazolium] solution
<b>DDS</b>	Drug delivery system
<b>DLS</b>	Dynamic light scattering
<b>EE%</b>	Encapsulation efficiency
<b>LDH</b>	Lactate dehydrogenase
<b>S-100</b>	Methacrylic acid copolymer
<b>NP</b>	Nanoparticles
<b>F127</b>	Pluronic F127
<b>PBMCs</b>	Peripheral blood mononuclear cells
<b>PLGA</b>	Poly(lactic- <i>co</i> -glycolic acid)
<b>PI</b>	Propidium iodide
<b>PrEP</b>	Pre-exposure prophylaxis
<b>SFS</b>	Semen fluid simulant
<b>TNF</b>	Tenofovir
<b>TDF</b>	Tenofovir disoproxil fumarate
<b>TEM</b>	Transmission electron microscopy
<b>TEER</b>	Transepithelial electrical resistance
<b>VFS</b>	Vaginal fluid simulant

## References

1. UNAIDS/WHO. Report on global AIDS epidemic. UNAIDS; Geneva: 2009. p. 362
2. Auvert B, Taljaard D, Lagarde E, Sobngwi-Tambekou J, Sitta R, Puren A. Randomized, controlled intervention trial of male circumcision for reduction of HIV infection risk: the ANRS 1265 Trial. *PLoS Med.* 2005; 2:e298. [PubMed: 16231970]
3. Pool R, Hart G, Green G, Harrison S, Nyanzi S, Whitworth J. Men's attitudes to condoms and female controlled means of protection against HIV and STDs in south-western Uganda. *Cult Health Sex.* 2000; 2:197–211. [PubMed: 12295882]
4. Chattopadhyay N, Zastre J, Wong HL, Wu XY, Bendayan R. Solid lipid nanoparticles enhance the delivery of the HIV protease inhibitor, atazanavir, by a human brain endothelial cell line. *Pharm Res.* 2008; 25:2262–2271. [PubMed: 18516666]
5. Asasutjarit R, Lorenzen SI, Sirivichayakul S, Ruxrungham K, Ruktanonchai U, Ritthidej GC. Effect of solid lipid nanoparticles formulation compositions on their size, zeta potential and potential for in vitro pHIS-HIV-hugag transfection. *Pharm Res.* 2007; 24:1098–1107. [PubMed: 17385021]
6. Baert L, van't Klooster G, Dries W, Francois M, Wouters A, Basstanie E, Iterbeke K, Stappers F, Stevens P, Schueller L, Van Remoortere P, Kraus G, Wigerinck P, Rosier J. Development of a long-acting injectable formulation with nanoparticles of rilpivirine (TMC278) for HIV treatment. *Eur J Pharm Biopharm.* 2009; 72:502–508. [PubMed: 19328850]
7. Mauck CK, Weiner DH, Creinin MD, Barnhart KT, Callahan MM, Bax R. A randomized Phase I vaginal safety study of three concentrations of C31G vs. Extra Strength Gynol II. *Contraception.* 2004; 70:233–240. [PubMed: 15325893]

8. Veazey RS, Klasse PJ, Schader SM, Hu Q, Ketas TJ, Lu M, Marx PA, Dufour J, Colonna RJ, Shattock RJ, Springer MS, Moore JP. Protection of macaques from vaginal SHIV challenge by vaginally delivered inhibitors of virus-cell fusion. *Nature*. 2005; 438:99–102. [PubMed: 16258536]
9. Dubey V, Mishra D, Nahar M, Jain V, Jain NK. Enhanced transdermal delivery of an anti-HIV agent via ethanolic liposomes. *Nanomedicine*. 2010; 6:590–596. [PubMed: 20093197]
10. Goddeeris C, Willems T, Houthoofd K, Martens JA, Van den Mooter G. Dissolution enhancement of the anti-HIV drug UC 781 by formulation in a ternary solid dispersion with TPGS 1000 and Eudragit E100. *Eur J Pharm Biopharm*. 2008; 70:861–868. [PubMed: 18691650]
11. Karim QA, Karim SS, Frohlich JA, Grobler AC, Baxter C, Mansoor LE, Kharsany AB, Sibeko S, Mlisana KP, Omar Z, Gengiah TN, Maarschalk S, Arulappan N, Mlotshwa M, Morris L, Taylor D. Effectiveness and Safety of Tenofovir Gel, an Antiretroviral Microbicide, for the Prevention of HIV Infection in Women. *Science*. 2010
12. Johnson TJ, Gupta KM, Fabian J, Albright TH, Kiser PF. Segmented polyurethane intravaginal rings for the sustained combined delivery of antiretroviral agents dapivirine and tenofovir. *Eur J Pharm Sci*. 2010; 39:203–212. [PubMed: 19958831]
13. Parikh UM, Dobard C, Sharma S, Cong ME, Jia H, Martin A, Pau CP, Hanson DL, Guenther P, Smith J, Kersh E, Garcia-Lerma JG, Novembre FJ, Otten R, Folks T, Heneine W. Complete protection from repeated vaginal simian-human immunodeficiency virus exposures in macaques by a topical gel containing tenofovir alone or with emtricitabine. *J Virol*. 2009; 83:10358–10365. [PubMed: 19656878]
14. Carballo-Dieguez A, Balan IC, Morrow K, Rosen R, Mantell JE, Gai F, Hoffman S, Maslankowski L, El-Sadr W, Mayer K. Acceptability of tenofovir gel as a vaginal microbicide by US male participants in a Phase I clinical trial (HPTN 050). *AIDS Care*. 2007; 19:1026–1031. [PubMed: 17852000]
15. Woolfson AD, Umrethia ML, Kett VL, Malcolm RK. Freeze-dried, mucoadhesive system for vaginal delivery of the HIV microbicide, dapivirine: optimisation by an artificial neural network. *Int J Pharm*. 2010; 388:136–143. [PubMed: 20045043]
16. Morrow RJ, Woolfson AD, Donnelly L, Curran R, Andrews G, Katinger D, Malcolm RK. Sustained release of proteins from a modified vaginal ring device. *Eur J Pharm Biopharm*. 2011; 77:3–10. [PubMed: 21055465]
17. Garg S, Vermani K, Garg A, Anderson RA, Rencher WB, Zaneveld LJ. Development and characterization of bioadhesive vaginal films of sodium polystyrene sulfonate (PSS), a novel contraceptive antimicrobial agent. *Pharm Res*. 2005; 22:584–595. [PubMed: 15846466]
18. du Toit LC, Pillay V, Choonara YE. Nano-microbicides: challenges in drug delivery, patient ethics and intellectual property in the war against HIV/AIDS. *Adv Drug Deliv Rev*. 2010; 62:532–546. [PubMed: 19922751]
19. Mamo T, Moseman EA, Kolishetti N, Salvador-Morales C, Shi J, Kuritzkes DR, Langer R, von Andrian U, Farokhzad OC. Emerging nanotechnology approaches for HIV/AIDS treatment and prevention. *Nanomedicine (Lond)*. 2010; 5:269–285. [PubMed: 20148638]
20. Ham AS, Cost MR, Sassi AB, Dezzutti CS, Rohan LC. Targeted delivery of PSC-RANTES for HIV-1 prevention using biodegradable nanoparticles. *Pharm Res*. 2009; 26:502–511. [PubMed: 19002569]
21. Woodrow KA, Cu Y, Booth CJ, Saucier-Sawyer JK, Wood MJ, Saltzman WM. Intravaginal gene silencing using biodegradable polymer nanoparticles densely loaded with small-interfering RNA. *Nat Mater*. 2009; 8:526–533. [PubMed: 19404239]
22. Owen DH, Katz DF. A review of the physical and chemical properties of human semen and the formulation of a semen simulant. *J Androl*. 2005; 26:459–469. [PubMed: 15955884]
23. Gupta KM, Barnes SR, Tangaro RA, Roberts MC, Owen DH, Katz DF, Kiser PF. Temperature and pH sensitive hydrogels: an approach towards smart semen-triggered vaginal microbicidal vehicles. *J Pharm Sci*. 2007; 96:670–681. [PubMed: 17154368]
24. Jiao Y, Ubrich N, Marchand-Arvier M, Vigneron C, Hoffman M, Lecompte T, Maincent P. In vitro and in vivo evaluation of oral heparin-loaded polymeric nanoparticles in rabbits. *Circulation*. 2002; 105:230–235. [PubMed: 11790706]

25. Dillen K, Bridts C, Van der Veken P, Cos P, Vandervoort J, Augustyns K, Stevens W, Ludwig A. Adhesion of PLGA or Eudragit/PLGA nanoparticles to Staphylococcus and Pseudomonas. *Int J Pharm.* 2008; 349:234–240. [PubMed: 17888598]
26. Dillen K, Vandervoort J, Van den Mooter G, Ludwig A. Evaluation of ciprofloxacin-loaded Eudragit RS100 or RL100/PLGA nanoparticles. *Int J Pharm.* 2006; 314:72–82. [PubMed: 16600538]
27. Basarkar A, Singh J. Poly (lactide-co-glycolide)-polymethacrylate nanoparticles for intramuscular delivery of plasmid encoding interleukin-10 to prevent autoimmune diabetes in mice. *Pharm Res.* 2009; 26:72–81. [PubMed: 18779928]
28. Glowka E, Sapin-Minet A, Leroy P, Lulek J, Maincent P. Preparation and in vitro-in vivo evaluation of salmon calcitonin-loaded polymeric nanoparticles. *J Microencapsul.* 2010; 27:25–36. [PubMed: 19229671]
29. Cetin M, Atila A, Kadioglu Y. Formulation and in vitro characterization of Eudragit(R) L100 and Eudragit(R) L100-PLGA nanoparticles containing diclofenac sodium. *AAPS Pharm Sci Tech.* 2010; 11:1250–1256.
30. Jain D, Panda AK, Majumdar DK. Eudragit S100 entrapped insulin microspheres for oral delivery. *AAPS Pharm Sci Tech.* 2005; 6:E100–107.
31. Murakami H, Kobayashi M, Takeuchi H, Kawashima Y. Preparation of poly(DL-lactide-co-glycolide) nanoparticles by modified spontaneous emulsification solvent diffusion method. *Int J Pharm.* 1999; 187:143–152. [PubMed: 10502620]
32. Owen DH, Katz DF. A vaginal fluid simulant. *Contraception.* 1999; 59:91–95. [PubMed: 10361623]
33. Tsukatani T, Suenaga H, Higuchi T, Akao T, Ishiyama M, Ezoe K, Matsumoto K. Colorimetric cell proliferation assay for microorganisms in microtiter plate using water-soluble tetrazolium salts. *J Microbiol Methods.* 2008; 75:109–116. [PubMed: 18586343]
34. Jorgenson, JH.; Turnidge, JD.; Washington, JA. Antibacterial susceptibility tests: dilution and disk diffusion methods. In: Murray, PR.; Baron, EJ.; Tenover, FC.; Tenover, FC.; Tenover, FC.; Tenover, FC.; Tenover, FC.; Tenover, FC.; Tenover, FC.; Tenover, FC.; Tenover, FC., editors. *Manual of clinical microbiology.* ASM Press; Washington DC: 1999.
35. Xie J, Wang CH. Self-assembled biodegradable nanoparticles developed by direct dialysis for the delivery of paclitaxel. *Pharm Res.* 2005; 22:2079–2090. [PubMed: 16132339]
36. Douglas KL, Piccirillo CA, Tabrizian M. Cell line-dependent internalization pathways and intracellular trafficking determine transfection efficiency of nanoparticle vectors. *Eur J Pharm Biopharm.* 2008; 68:676–687. [PubMed: 17945472]
37. Ibrahim HK, El-Leithy IS, Makky AA. Mucoadhesive nanoparticles as carrier systems for prolonged ocular delivery of gatifloxacin/prednisolone bitherapy. *Mol Pharm.* 2010; 7:576–585. [PubMed: 20163167]
38. Desai MP, Labhasetwar V, Amidon GL, Levy RJ. Gastrointestinal uptake of biodegradable microparticles: effect of particle size. *Pharm Res.* 1996; 13:1838–1845. [PubMed: 8987081]
39. Choi SU, Bui T, Ho RJ. pH-dependent interactions of indinavir and lipids in nanoparticles and their ability to entrap a solute. *J Pharm Sci.* 2008; 97:931–943. [PubMed: 17546665]
40. UFA Administration. FDA Viread prescribing information. 2008.
41. Klose D, Siepmann F, Elkharraz K, Siepmann J. PLGA-based drug delivery systems: importance of the type of drug and device geometry. *Int J Pharm.* 2008; 354:95–103. [PubMed: 18055140]
42. Badawy SI, Hussain MA. Microenvironmental pH modulation in solid dosage forms. *J Pharm Sci.* 2007; 96:948–959. [PubMed: 17455349]
43. Li L, Schwendeman SP. Mapping neutral microclimate pH in PLGA microspheres. *J Control Release.* 2005; 101:163–173. [PubMed: 15588902]
44. Nguyen DA, Fogler HS. Facilitated diffusion in the dissolution of carboxylic polymers. *AIChE Journal.* 2005; 51:415–425.
45. Tevi-Benissan C, Belec L, Levy M, Schneider-Fauveau V, Si Mohamed A, Hallouin MC, Matta M, Gresenguet G. In vivo semen-associated pH neutralization of cervicovaginal secretions. *Clin Diagn Lab Immunol.* 1997; 4:367–374. [PubMed: 9144379]
46. Zolnik BS, Burgess DJ. Effect of acidic pH on PLGA microsphere degradation and release. *J Control Release.* 2007; 122:338–344. [PubMed: 17644208]

47. Houchin ML, Neuenswander SA, Topp EM. Effect of excipients on PLGA film degradation and the stability of an incorporated peptide. *J Control Release*. 2007; 117:413–420. [PubMed: 17207882]
48. Mu L, Feng SS. A novel controlled release formulation for the anticancer drug paclitaxel (Taxol): PLGA nanoparticles containing vitamin E TPGS. *J Control Release*. 2003; 86:33–48. [PubMed: 12490371]
49. Lee WA, He GX, Eisenberg E, Cihlar T, Swaminathan S, Mulato A, Cundy KC. Selective intracellular activation of a novel prodrug of the human immunodeficiency virus reverse transcriptase inhibitor tenofovir leads to preferential distribution and accumulation in lymphatic tissue. *Antimicrob Agents Chemother*. 2005; 49:1898–1906. [PubMed: 15855512]
50. Sassi AB, Isaacs CE, Moncla BJ, Gupta P, Hillier SL, Rohan LC. Effects of physiological fluids on physical-chemical characteristics and activity of topical vaginal microbicide products. *J Pharm Sci*. 2008; 97:3123–3139. [PubMed: 17922539]
51. Mahalingam A, Smith E, Fabian J, Damian FR, Peters JJ, Clark MR, Friend DR, Katz DF, Kiser PF. Design of a semisolid vaginal microbicide gel by relating composition to properties and performance. *Pharm Res*. 2010; 27:2478–2491. [PubMed: 20842411]
52. Lederman MM, Offord RE, Hartley O. Microbicides and other topical strategies to prevent vaginal transmission of HIV. *Nat Rev Immunol*. 2006; 6:371–382. [PubMed: 16639430]
53. Rohan LC, Moncla BJ, Kunjara Na Ayudhya RP, Cost M, Huang Y, Gai F, Billitto N, Lynam JD, Pryke K, Graebing P, Hopkins N, Rooney JF, Friend D, Dezzutti CS. In vitro and ex vivo testing of tenofovir shows it is effective as an HIV-1 microbicide. *PLoS One*. 2010; 5:e9310. [PubMed: 20174579]
54. Fichorova RN, Bajpai M, Chandra N, Hsiu JG, Spangler M, Ratnam V, Doncel GF. Interleukin (IL)-1, IL-6, and IL-8 predict mucosal toxicity of vaginal microbicide contraceptives. *Biol Reprod*. 2004; 71:761–769. [PubMed: 15128598]
55. Fichorova RN, Anderson DJ. Differential expression of immunobiological mediators by immortalized human cervical and vaginal epithelial cells. *Biol Reprod*. 1999; 60:508–514. [PubMed: 9916021]
56. Garg S, Tambweker KR, Vermani K, Garg A, Kaul CL, Zaneveld LJ. Compendium of pharmaceutical excipients for vaginal formulations *Pharm Technol Drug Deliv*. 2001; 11:14–24.
57. Klebanoff SJ, Coombs RW. Viricidal effect of *Lactobacillus acidophilus* on human immunodeficiency virus type 1: possible role in heterosexual transmission. *J Exp Med*. 1991; 174:289–292. [PubMed: 1647436]
58. Wilks M, Wiggins R, Whiley A, Hennessy E, Warwick S, Porter H, Corfield A, Millar M. Identification and H<sub>2</sub>O<sub>2</sub> production of vaginal lactobacilli from pregnant women at high risk of preterm birth and relation with outcome. *J Clin Microbiol*. 2004; 42:713–717. [PubMed: 14766841]
59. Rejman J, Oberle V, Zuhorn IS, Hoekstra D. Size-dependent internalization of particles via the pathways of clathrin- and caveolae-mediated endocytosis. *Biochem J*. 2004; 377:159–169. [PubMed: 14505488]

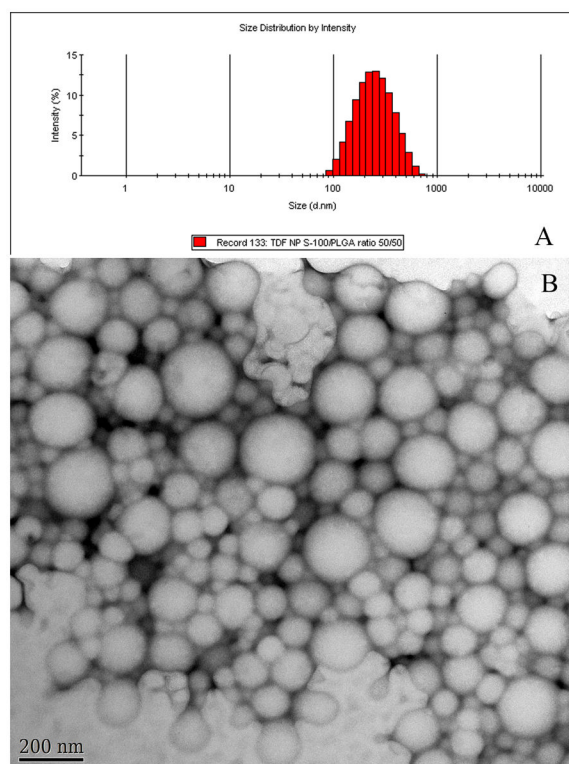


**Fig. 1.** (A) Size distribution by volume of tenofovir disoproxil fumarate loaded nanoparticle prepared with PLGA/S-100 in 50/50 weight ratio measured by dynamic light scattering. (B) Typical transmission electron micrograph (Bar=200 nm).



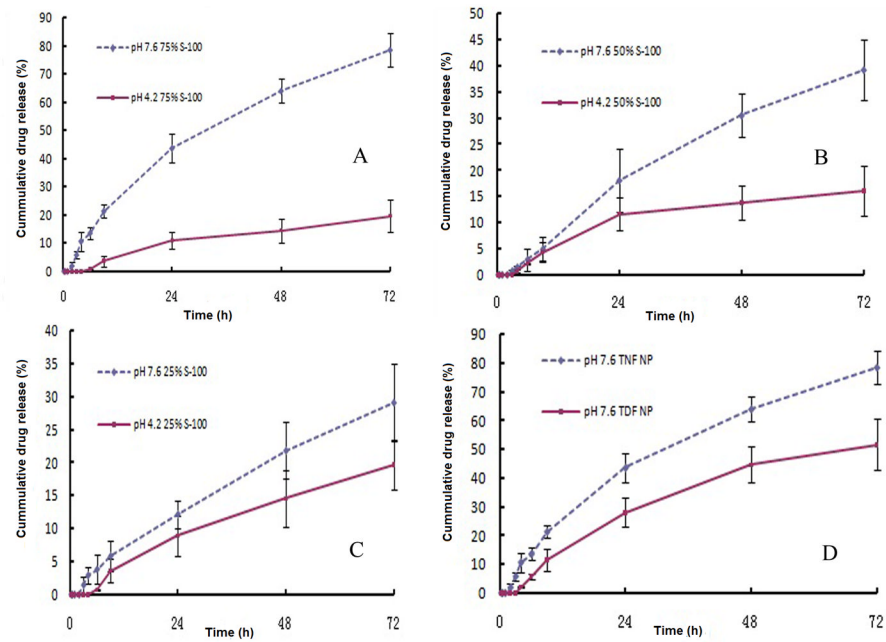


**Fig. 2.** *in vitro* release profile at pH=4.2 (solid line) and pH=7.6 (dash line) of TNF loaded NP prepared with different weight ratio of S-100 to PLGA, n=3. (A) 75% S-100. (B) 50% S-100. (C) 25% S-100. (D) Comparative *in vitro* release profile of 75% S-100 NP encapsulated with TNF or TDF under 37°C at pH=7.6, n=3.

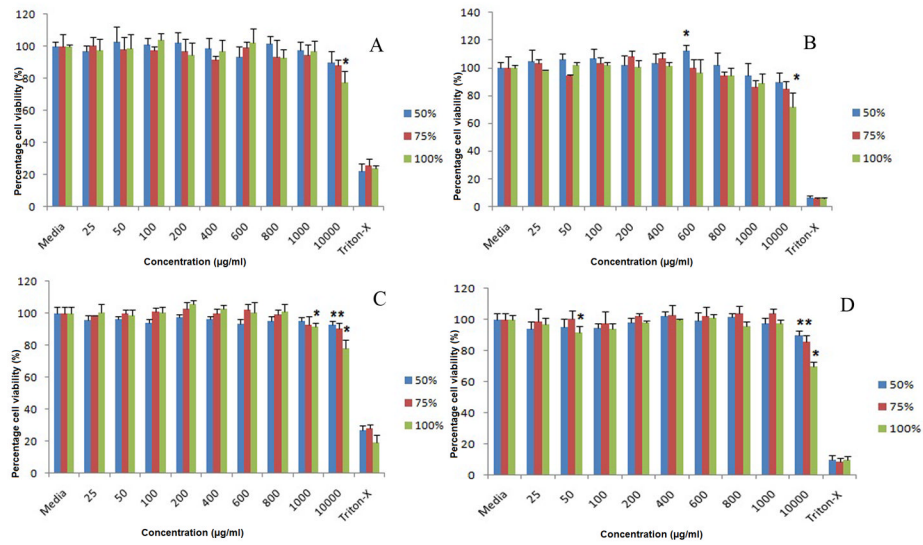


**Fig. 3.** MTS assay of VK and Endo cells after treated with PLGA/S-100 NP (S-100 at 50%, 75% and 100% w/w) at various concentrations. (A) VK cells at 24 hr, (B) VK cells at 48 hr, (C) Endo cells at 24 hr, (D) Endo cells at 48 hr. The data shown represent the mean  $\pm$  standard deviation of 3 independent experiments,  $n=3$ . Stars indicate significant differences from the controls, with  $P<0.05$ .

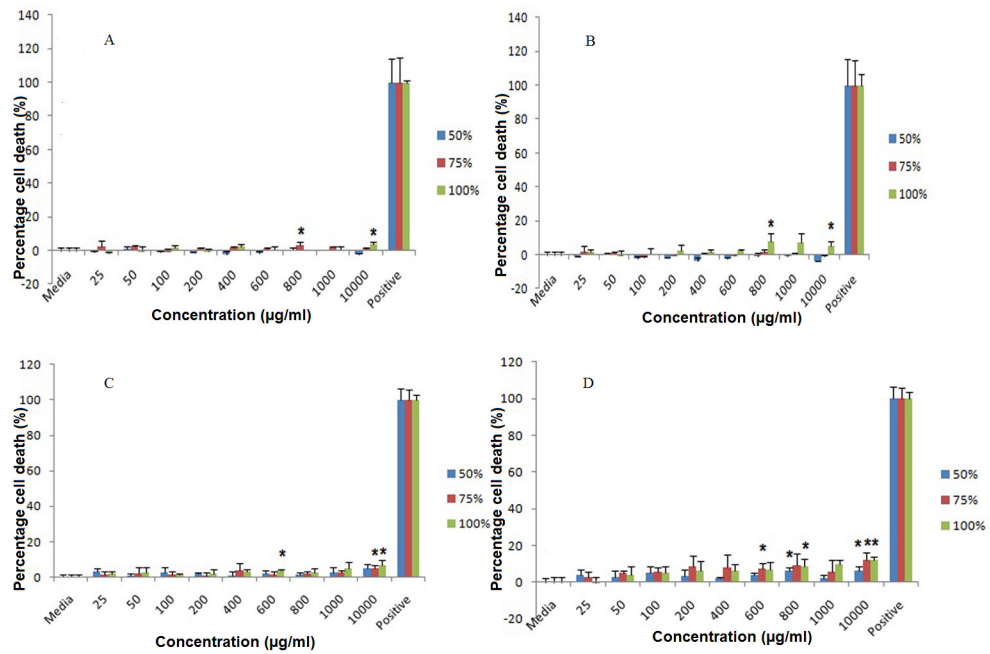


**Fig. 4.** LDH assay of PLGA/S-100 NP on VK and Endo cells at various concentrations. (A) VK cells at 24 hr, (B) VK cells at 48 hr, (C) Endo cells at 24 hr, (D) Endo cells at 48 hr. The data shown represent the mean  $\pm$  standard deviation of 3 independent experiments,  $n=3$ . Stars indicate significant differences from the controls, with  $P<0.05$ .

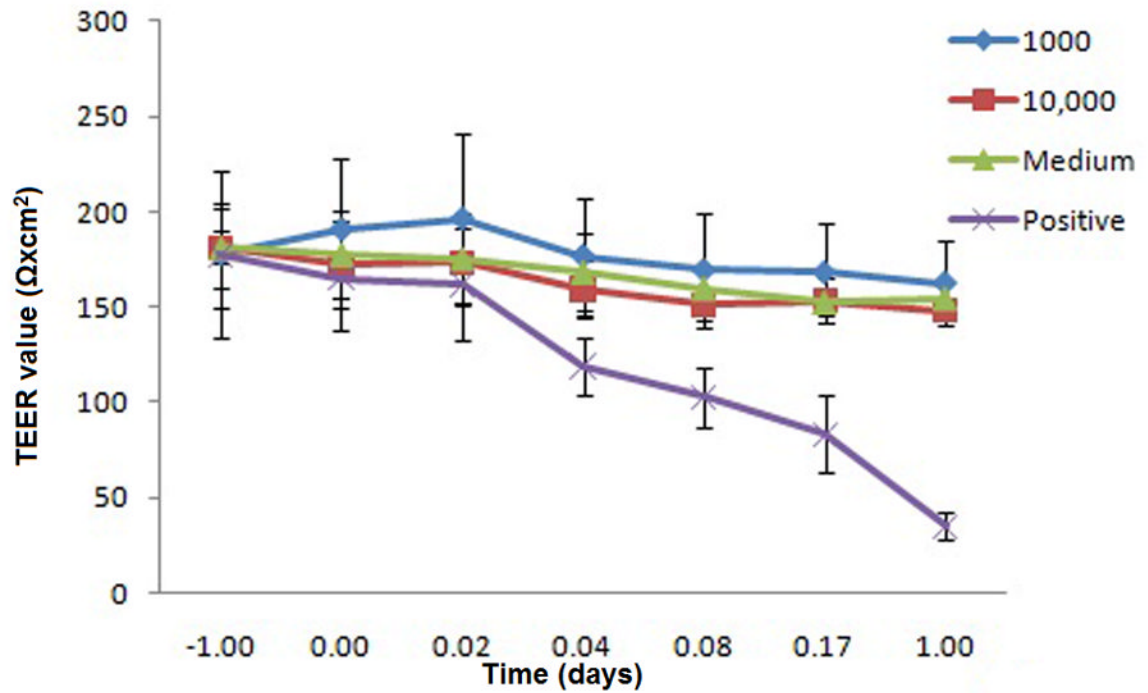


**Fig. 5.** Effect of PLGA/S-100 NP on Endo cells monolayer integrity. Endo cells were grown in transwell supports and resistance readings were measured at 30 min, 1, 2, 4, and 24 hr. The data shown represent the mean  $\pm$  standard deviation of 3 independent experiments, n=3.

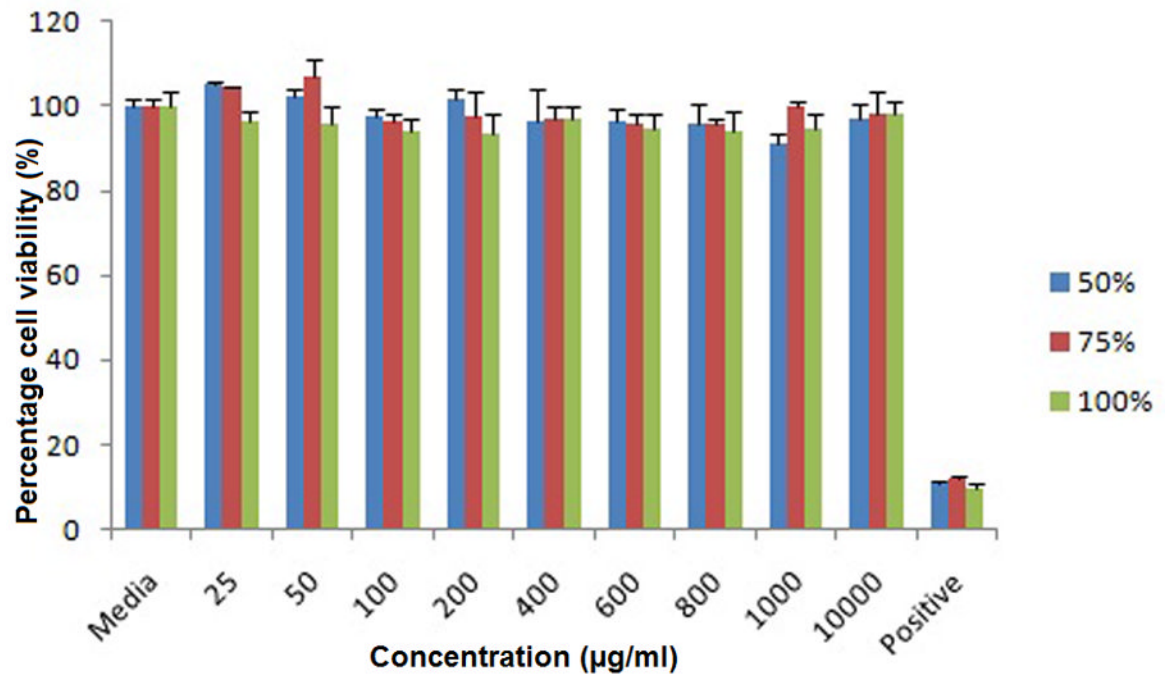


**Fig. 6.** Viability of *Lactobacillus crispatus* treated with PLGA/S-100 NP (S-100 at 50%, 75% and 100% w/w) after 48 hrs at various concentrations. The data shown represent the mean  $\pm$  standard deviation of 3 independent experiments, n=3.

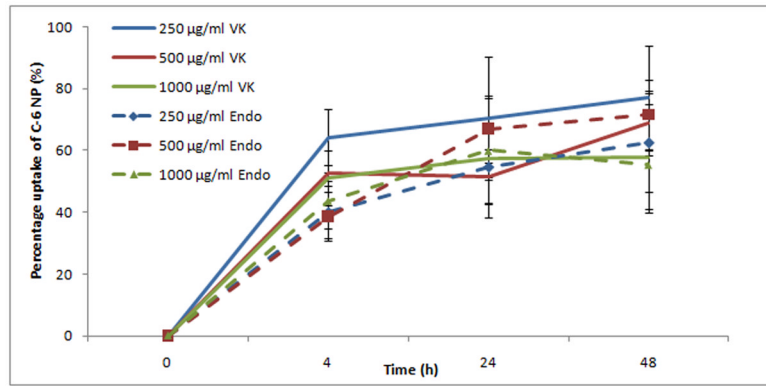


**Fig. 7.** Time dependent uptake efficiency of the nanoparticles by two vagina epithelial cell lines (VK and Endo). Each data point shown is the average of three samples. The data shown represent the mean  $\pm$  standard deviation of 3 independent experiments, n=3.

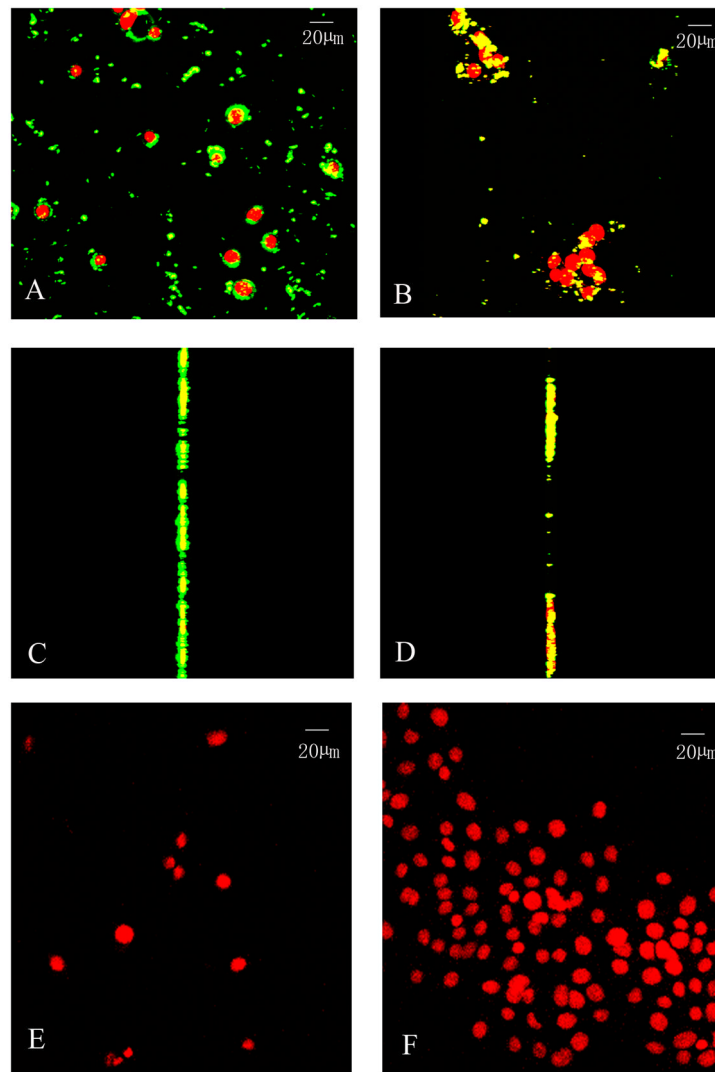


**Fig. 8.** Confocal fluorescence images of VK and Endo cells with coumarin-6 encapsulated PLGA/S-100 50%/50% NP (C-6 NP) after 4 hr incubation and control. An overlay of red and green channels is shown. (A) Z-stacking of X–Y projection of VK cells treated with C-6 NP. (B) Z-stacking of X–Y projection of Endo cells treated with C-6 NP. (C) Y–Z projection of the optical section of the VK cells incubated with C-6 NP. (D) Y–Z projection of the Endo cells incubated with C-6 NP. (E) Z- stacking of X–Y projection of control VK cells treated with medium alone. (F) Z-stacking of X–Y projection of control Endo cells treated with medium alone.

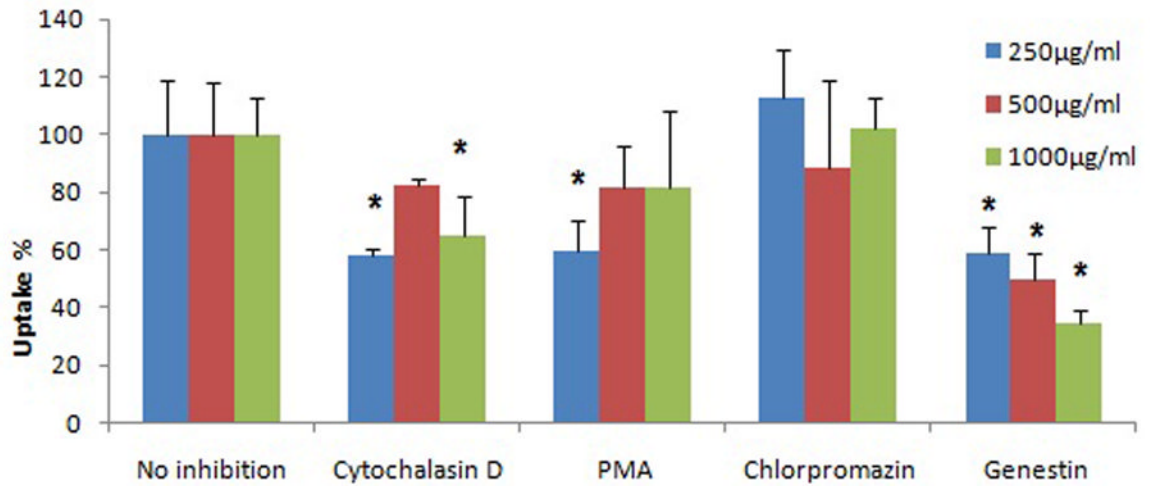


**Fig. 9.** Effects of inhibitors on the internalization of C-6 NP on VK cells. For all treatments, cells are pre-treated 30 min with the inhibitor prior to treatment with C-6 NP. After 24 h, cells were analyzed by microplate reader. Values indicate means  $\pm$  standard deviation of 3 independent experiments,  $n=3$ . Stars indicate significant differences from the controls, with  $P<0.05$ .



Table 1

Physicochemical characterization of TNF and TDF loaded pH-responsive nanoparticles<sup>a</sup>

Drug (5 mg)	S100/PLGA ratio	Particle size before freeze drying (nm)	Particle size after freeze drying (nm)	EE (%)	Drug loading (% w/w)	PDI	Z-potential (mV)
TNF	25/75	240.0±16.9	315.6±24.1	15.4±1.2	0.77±0.06	0.206±0.021	-3.35±0.31
TNF	50/50	225.2±16.5	336.2±18.9	16.1±1.0	0.81±0.05	0.224±0.032	-2.09±0.12
TNF	75/25	298.0±14.9	501.7±44.5	9.5±1.9	0.48±0.10	0.269±0.094	-3.26±0.25
TDF	25/75	226.1±13.5	310.6±29.1	37.2±3.9*	1.86±0.19*	0.219±0.032	-3.37±0.50
TDF	50/50	251.1±27.0	301.5±47.6	26.9±1.4**	1.34±0.07**	0.190±0.046	-3.87±0.28
TDF	75/25	336.8±41.4	433.6±36.2	24.0±1.6***	1.20±0.08***	0.278±0.068	-2.38±0.33

<sup>a</sup>Each data point shown is the average of three samples (n=3)\*, \*\*, \*\*\* Statistical significant difference ( $P < 0.05$ ) between means of TNF and TDF groups.